STUDY OF PREMIXED FLAME/FLOW INTERACTION UNDER A FLOW OSCILLATION

Byung-Il Choi and Hyun-Dong Shin
Department of Mechanical Engineering
Korea Advanced Institute and Science and Technology
Kusong-Dong, Yusong-gu, Taejon, 305-701, KOREA

ABSTRACT

In wrinkled flamelet regime of turbulent combustion, the reacting front in turbulent combustion is considered as a very thin interface between two non-reactive flows. Properties of the flame front remain unchanged from the laminar flame and the flame front is only wrinkled by the flow field. The resulting motion is mainly affected by the hydrodynamic interaction that makes the flow field be dependent on the wrinkled front. Numerical and experimental studies on the wrinkled flame front have been conducted in order to examine the flame/flow interaction in the time varying flow field. A flame model where the flame is regarded as a source of volume and vorticity. The flame surface is determined by conventional G-equation. To confirm the numerical simulation, the flame front behavior under the oscillating flow field is observed experimentally. From the results of numerical simulation and the experimental observation, it is clearly found that the upstream flow characteristics are modified by the motion of the curved flame front and that the hydrodynamic interaction between flame and flow results from the volume generation and vorticity production at the flame front. The vorticity production is found to be an integral part of velocity field, especially in time varying flow.

INTRODUCTION

Gas flows associated with the combustion processes occurring in engineering device are turbulent. These turbulent reacting flows are far from being fully understood because of strong non-linearity in chemical reaction. Chemical reaction occurs in a distributed reaction zone for some specific conditions, but in almost conditions, intensely in a flame front which is represented by the deflagration wave (Poinsot *et al.*, 1991). These flame fronts propagate with a subsonic speed into frozen mixtures through the diffusive transport processes of mass and energy. The gas density varies across the flame front of which thickness is usually much smaller than the characteristic scale of the gas flow. Thus the flame front can be considered as a hydrodynamic discontinuity between reactants and products. The motion of the flame front results not only from the inner structure but also from the flow characteristics near the flame front. The inner structure controls the motion of the flame front relative to the flow, and the motion and shape of the flame front modify the flow characteristics due to the hydrodynamic interaction. These two effects have been studied separately such that convective effects and/or diffusive effects are neglected, respectively. Recently, Clavin and Willams (1982) developed the description method which consider the coupling of these two effects.

Since the heat release in real flames is very large, there is a considerable volume expansion across flame front. The motion and shape of flame front modify the flow field as a result of the volume expansion. In order to consider the active role of the flame front due to the volume generation, Uberoi (1963) and Ghoniem *et al.* (1982) simulated the flame motion in laminar and turbulent flow fields, respectively, regarding the flame front as a volume source. Ashurst (1987) extended the source model further to predict the flame motion and turbulent characteristics in turbulent V-shape and Bunsen flames, and showed that the source model is much coincident with experimental results. Recently, Pindra and Talbot (1988) showed that source-induced velocity exhibits singularities in the tangential component, and that the vorticity production at the flame front should be

considered to counteract the singularities in the source-induced velocity. Rhee *et al.* (1995) extended the vorticity production model of the Pindra and Talbot to simulate the motion of the turbulent V-shape flame. They showed that the volume generation plays a decisive role in determining the flame shape and the vorticity production has main effects in the prediction of the turbulent characteristics near the flame front.

The primary objective of the present study is to examine the mechanism of the hydrodynamic interaction between flame front and flow field. The authors simulate the motion of the wrinkled flame front in oscillating flow field where the effects of hydrodynamic interaction is amplified. Flame front is modeled as a surface at which the volume and vorticity are generated, and G-equation (Kerstein *et al.*, 1988) and discrete vortex method are used. Experiments are also conducted to confirm numerical simulation.

NUMERICAL STUDY

Governing Equation and Problem Definition

The flame is located in the 2-dimensional channel and the upstream flow is oscillating sinusoidally. The coordinate system and the flow geometry are shown in Figure 1.

The equations governing the motion of the flame front in the sinusoidal oscillating flow field are obtained under the following assumptions :

1) Flow field is 2-dimensional and inviscid ;
2) Ma number of the flow is small enough to make the compressible effects negligible in the burned and unburned region ;
3) The flame is considered as a thin interface separating reactants and products ;
4) The flame front propagates at a prescribed laminar burning velocity with respect to the reactants in the direction normal to its surface ;

The motion of the flame front can be described by so-called G equation.(Kerstein *et al.*, 1988) :

$$\left(\frac{dG}{dt}\right)_{flame} = \frac{\partial G}{\partial t} + \boldsymbol{u}\cdot\nabla G - S_u|\nabla G| = 0 \tag{1}$$

Here, $\boldsymbol{u}$ is the unburned flow velocity at the flame front, and S_u is the laminar burning velocity. The function G is chosen such that G<0 on the unburned region, G>0 on the burned region and G=0 on the flame front. Markstein relation for the laminar burning velocity, S_u, is used in the present study since it improves an intrinsic instability of flame front. (Markstein, 1964) :

$$S_u = S_u^o(1 - Lx) \tag{2}$$

Here S_u^o is the laminar burning velocity of an adiabatic planar flame, x is the curvature of the flame front and L is Markstein length scale. A more simple form of the governing equation is obtained by setting the G to be proportional to the distance from the flame front as follows :

$$G(x, y, t) = x - g(y, t) \tag{3}$$

Substituting for equations (2) and (3) in equation (1), we obtain the final form of the governing equation for the motion of the flame front as follows :

$$\frac{\partial g}{\partial t} = -u + v\frac{\partial g}{\partial y} + S_u^o(1 - Lx)\sqrt{1 + \left(\frac{\partial g}{\partial y}\right)^2} \tag{4}$$

Here, u and v are the velocity components in x and y directions, respectively. In the governing equation, the location of the flame front, $g(y, t)$ is determined by the flow velocity, (u, v) at the flame front and the shape parameters of the flame front, dg/dy and x. It should be noted that there is an flame/flow interaction through the flow velocity (u, v) in the governing equation implicitly. The flow field (u, v) convects the flame front and the flame front affects the flow field through thermal expansion and the vorticity production at the flame front. This effect of the flame front on the flow field will be described by a flame model.

Flame Model

In the present study, flame front is regarded as the sources of volume and vorticity (Pindra and Talbot, 1988).

Let S_u and S_b be the laminar burning velocity in the unburned and burned regions, respectively. The strength of volume source is associated with the increment of fluid velocity, say $m = S_b - S_u$. From the mass continuity, volume source is expressed as

$$m = S_b - S_u = \left(\frac{\rho_u - \rho_b}{\rho_b}\right)S_u = (\nu - 1)S_u \tag{5}$$

Here, ν is the density ratio across the flame front.

Pindra and Talbot (1988) explained the physical meaning of the vorticity production across the flame front. We adapt their idea and extend to the more general expression for vorticity production(Hayes, 1959) as follows :

$$\omega = \left(\frac{1}{\rho_b} - \frac{1}{\rho_u}\right)\frac{\partial(\rho_u S_u)}{\partial s} + \frac{\rho_u - \rho_b}{\rho_u S_u}\left\{\frac{d\,\boldsymbol{u}_s}{dt} + \boldsymbol{u}_s\cdot\frac{\partial\,\boldsymbol{u}_s}{\partial s} - V_n\frac{\partial V_n}{\partial s} - V_n\,\boldsymbol{u}_s\,x)\right\} \tag{6}$$

, where subscript n, s are the normal and tangential directions, respectively, d/dt the time derivative with respect to an observer who lies on the flame front and moves in a normal direction to the flame front as the flame front moves.

Flow Field Description

Since we consider the flame front as a volume source and a vorticity source, we decompose the resulting flow field $\boldsymbol{u}$ into three distinct components :

$$\boldsymbol{u} = u\boldsymbol{i} + v\boldsymbol{j} = \boldsymbol{u}_P + \boldsymbol{u}_{vol} + \boldsymbol{u}_{vor}$$

Here $\boldsymbol{u}_P$ is the potential velocity, $\boldsymbol{u}_{vol}$ the volume velocity due to the volume source, and $\boldsymbol{u}_{vor}$ the rotational velocity due to the flame generated vorticity.

In order to simulate the motion of the flame front in the sinusoidally oscillating flow field, we introduce a sinusoidally oscillating potential as follows :

$$\boldsymbol{u}_P = [u_{P,mean} + u_{P,a} \sin(2\pi f t)]\,\boldsymbol{i} \tag{7}$$

Complex potential is introduced to describe the velocity field due to the volume source. Consider a point source of which strength m in the 2-D channel whose width is 1.(see Figure 1) The point source gives rise to the outflow across the channel boundaries. To satisfy the impermeabilty condition at the wall boundaries, volume sources of which locations are symmetric to the both side walls have to be distributed infinitely as follows :

$$\begin{aligned} w_{vol}(z) &= \frac{m}{2\pi}\left[\frac{1}{z-\zeta} + \sum_{n=1}^{\infty}\frac{1}{z-(\zeta+2ni)} + \sum_{n=-1}^{-\infty}\frac{1}{z-(\zeta+2ni)}\right] \\ &+ \frac{m}{2\pi}\left[\frac{1}{z-\bar{\zeta}} + \sum_{n=1}^{\infty}\frac{1}{z-(\bar{\zeta}+2ni)} + \sum_{n=-1}^{-\infty}\frac{1}{z-(\bar{\zeta}+2ni)}\right] \\ &= -\frac{im}{4}\left[\cot\left\{\pi\frac{(z-\zeta)}{2i}\right\} + \cot\left\{\pi\frac{(z-\bar{\zeta})}{2i}\right\}\right] \end{aligned}$$

Here, $z = x + iy$ and ζ is the location of the volume source. Since the volume source is given by a line source, we can obtain the volume induced velocity field due to the line source by integrating the above equation as follows:

$$w_{vol}(z) = -\frac{m}{2\pi}\log\left[\sin\left\{\pi\frac{(z-\zeta)}{2i}\right\} + \sin\left\{\pi\frac{(z-\bar{\zeta})}{2i}\right\}\right]$$

In the present study, we assume that the unburned region is irrotational. However, the burned region is rotational because vorticity is produced at the flame front and convected towards the burned region. The vortical velocity field in the burned region is characterized by the locations and the circulations of the vortices generated at the flame front. The circulation of each vortex is expressed by the vorticity and the area of the vortex as $\Gamma = \omega \Delta A = \omega \nu \Delta l\, S_u \Delta t$, where the Δl is the length of the flame segment, ν the density ratio across the flame front, and Δt the numerical time step. The generated vortices at the flame front is simply convected by the flow velocity as follows :

$$\boldsymbol{x}_\omega(t+\Delta t) = \boldsymbol{x}_\omega(t) + \int_{\Delta t}\boldsymbol{u}(\boldsymbol{x}_\omega)\,dt \tag{8}$$

Vortices, which were convected from the flame front, induce the rotational velocity field. A vortex in computational domain also gives rise to the outflow across the wall boundaries. The velocity potential, which satisfies the impermeability condition, is obtained by the same procedure as the case of the volume source as follows :

$$w_{vor}(z) = \frac{\Gamma}{4}\left[\cot\left\{\pi\frac{(z-\zeta)}{2i}\right\} + \cot\left\{\pi\frac{(z-\bar{\zeta})}{2i}\right\}\right]$$

Numerical Method and Parameters

In the governing equation (4) for the motion of the flame front, the length and the velocity are nondimensionalized by the channel width H and the velocity laminar burning velocity S_u^o, respectively. The time is therefore nondimensionalized by the H/S_u^o. All the spatial derivatives in the governing equation (4) are centrally differenced and symmetric image to the wall is used in the wall boundary.

It has been known that the Markstein length scale L ranges from 2 to 6 times of the laminar flame thickness for hydrocarbon fuels (Garcia *et al.*, 1984). In the present study, L is set to 3mm assuming that the thickness of the laminar flame is 0.5mm and its nondimensionalized value is 0.06. The density ratio ν across the flame front is 5, which represents lean hydrocarbon flames.

The sinusoidal flow oscillation is obtained through the sinusoidal potential component as equation (7). The nondimensionalized frequency of the flow oscillation is 15 and the amplitude of the flow oscillation is set to 1.5 times of the laminar burning velocity. The wall condition is given to Neumann boundary, which is satisfied intrinsically in the flow field description as previously described.

Initially the whole flow field is irrotational, and the burned region becomes rotational due to the vorticity rhat is generated at the flame front. Vortices are produced at each time step and injected towards the burned region, and are convected by the equation (8). The computation is continued until the periodic solutions for the motion of the flame front are obtained.

EXPERIMENTAL STUDY

The experimental study on motions of the premixed under the flow oscillation is carried out to make comparisons with the numerical results.

The experimental burner is composed of a pyrex tube and a plenum chamber located under the tube. The tube where the curved flame is located is 47mm in diameter and 1.2m in length. Lean propane/air mixture whose equivalence ratio is 0.56 provided from the base of the tube and flows through the tube with a mean velocity 0.17m/sec. Sinusoidal flow oscillation is obtained acoustically using the loud speaker located in the plenum chamber. The frequency and the amplitude of the flow oscillation are 30Hz and 0.17m/sec, respectively. The

Table 1. The numerical and experimental parameters

	Dimension	S_u°	Oscillating amplitude	Nondimensional frequency	Density ratio
Numerical simulation	47mm (Channel Width)	0.1 m/s	1.5 S_u°	15	5
Experiment	50mm (Tube Diameter)	0.113 m/s	1.45 S_u°	12.5	5.5

amplitude of the flow oscillation is about 1.45 times of the laminar burning velocity of the mixture. The wavelength corresponding the oscillating frequency is enough longer than the diameter of the tube and hence it is possible to make the flow oscillation be uniform except near the tube wall. A LDV system is used in conjunction with the phase averaging technique to measure the flow velocity near the flame front. It is found that the velocity oscillation at far upstream is nearly uniform except the vicinity of the wall and that this oscillating condition is similar to that of the numerical study.

Triggered ICCD camera system is utilized to visualize the instantaneous flame motion and pathlines of the fluid particles

RESULTS AND DISCUSSION

We are to describe the effects of the flame motion on the flow field by comparing the numerical results with the experimental results in the oscillating flow field. Table 1. shows the parameters used in both the numerical simulation and the experiment.

The periodic motion of the flame front and the overall flow characteristics are depicted in Figure 2. Figure 2(a) shows the numerical results containing the flame shape, the pathlines of the fluid particles and the flame generated vortices. It is found that the numerical result is very similar to the experimental result shown in Figure 2(b). It is remarkable that the pathlines are abruptly deflected to horizontally in the unburned region whereas the horizontal component of the potential velocity is not varied. This abrupt deflection of the pathlines might be explained by the moving of the volume source. The oscillation of the vertical component of the potential velocity make the flame front oscillate in vertically. Since the flame front is inclined, the resulting motion of the flame front induces the oscillation of the source-induced velocity in normal direction to the flame front. As shown in the Figure, the magnitude of the deflection is therefore proportional to the inverse of the distance from the flame front, which is inherent in the source representation. These results on the pathlines clarify that the volume expansion across the flame front has to be considered in the simulation of the flame motion. The flame-generated vortices are also displayed in Figure 2(a) at the phase of 0° with respect to the velocity oscillation. These vortices are generated at the flame front and convected by the flow velocity as previously described. The vortices of positive and negative circulations are marked by the filled and open circles, respectively. The only 7 percents of about 10000 vortices are displayed for simplicity. It is shown that the signs of the circulation of the vortices are stratified spatially and symmetric to the line of the center since the flame shape and the flow field are symmetric. The region where the vortices are stratified corresponds to a half period of the flow oscillation. It will be demonstrated later in detail that the stratification of the vortices makes a decisive role in determining the motion of the flame front.

The resulting motion of the flame front at each phase of the flow oscillation is displayed in Figure 3. The flame front oscillates periodically in vertical direction. If the motion of the flame front does not affect the flow field (passive propagation), the magnitude of the flame oscillation is expected to be constant along the flame front and may be expressed as $\int_0^{T/2} u_{p,a} \sin 2\pi ftdt$. These values are about 0.03 in numerical case and 1.6 mm in experimental case, respectively. It is very noticeable that the amplitude of the flame oscillation near the wall is larger than that of passive propagation but the amplitude near the flame center is very small (numerical) and nearly zero (experimental). These motions of the flame front near the flame center imply that the active effects of the flame front on the flow field have to be considered in the numerical simulation of the curved flame front.

Figure 4 shows the variation of the total velocity in unburned region along the centerline. In the Figure, x_m means the distance from the flame front. In the numerical result, the flow velocity at the far upstream (x_m=10) oscillates with an amplitude of $1.5S_L$ as given in potential component and its amplitude is decreased gradually with decreasing x_m. At the bottom of the flame front (x_m=0.001) the amplitude of the flow velocity is only about 30 percents of the far upstream. The reduction of the velocity oscillation is also found in the experimental result although the velocity at the bottom of the flame front is not measured. The motion of the flame front near the flame center (Figure 3) is thought to be originated from the reduction of the velocity oscillation.

A plausible explanation on the reason why the reduction of the velocity oscillation occurs, can be drawn through the vorticity production at the flame front. Since the velocity due to the volume source is dependent only on the shape of the flame front and the variation of the flame shape during a period of the velocity oscillation is small, the velocity field due to the volume source cannot explain the reduction of the oscillating velocity. It was showed that the sign of the vorticity is stratified in Figure 2. The stratification of the vorticity can be

explained if the vorticity having the different sign is produced at the flame front with the phase of the velocity oscillation.

Figure 5 shows the magnitude of the vorticity as the function of the phase which is produced at the left side of the flame (y=0.35) as the function of the phase. The vorticity is produced by five different mechanisms from the Hayes' expression (equation (6)). We call them as steady, unsteady, strain, rotation and curvature terms, respectively.

The vorticity production due to the steady term is nearly constant during a period of the velocity oscillation, provide that the laminar burning velocity S_u is dependent on the shape of the flame front by the Markstein relation. The vorticity production due to the flow strain, the rotation of the flame front and movement of flame front with curvature are negligible in comparison with the total production. When the velocity oscillation is given in the flow field, it is remarkable that the sign and magnitude of the produced vorticity are almost dependent on the unsteady term that results from the variation of the tangential velocity along the flame front. The oscillating velocity given by the potential component induces the time variation of the tangential velocity since the flame front is inclined. At the left side of the flame front (y=0.35) the time derivative of the tangential velocity has the opposite sign of the time derivative of the given potential velocity. When the oscillating velocity in potential component is increased (0^o-90^o and 270^o-360^o), the vorticity produced at the flame front has the negative sign that implies the clockwise rotation. The negative vorticity counteracts the increasing potential velocity near the flame center because it induces the negative rotational velocity. The vorticity produced at the flame front has the positive sign with the decrease of the oscillating velocity in potential component (90^o-270^o). The positive vorticity counteracts the decreasing potential velocity near the flame center since it induces the positive rotational velocity.

These effects of the flame-generated vorticity on the flow field are clearly seen in Figure 6. Figure 6 shows the rotational velocity field due to the flame-generated vorticity at various phases of the velocity oscillation. At the phase of 90^o (Figure 6(a)) when the velocity oscillation has positive maximum magnitude, the negative vortices, which were produced during -90^o~-90^o, are widely distributed near the flame front and dominate the velocity field. The negative velocity due to the strong vortical field is enough large to counteract the increased potential velocity. At the phase of 270^o (Figure 6(b)) when the velocity oscillation has negative maximum magnitude, the vortices, which were produced during 90^o~270^o, are distributed in the region between the flame front and the strong negative vortices, which were produced during -90^o~90^o. The vortical field induces much smaller negative velocity than that of phase 0^o and counteracts the decreased potential velocity. From the results on the vortical fields at various phases, it is clearly shown that the vortical flow field due to the flame-generated vorticity counteracts the oscillating velocity near the curved flame front and that notable phenomena on the flame motion near the flame center as shown in Figure 3 results from the flame-generated vorticity.

CONCLUSION

The numerical and experimental works have been conducted to investigate the flame/flow interaction in oscillating flow field.

Volume generation at the flame front reorganizes the flow field near the flame front and overall flow characteristics such as pathlines of fluid particles is explained successfully through the volume source. The vorticity production is mainly dependent on the unsteady term due to time varying flow field and the vortical flow field due to the flame generated vorticity is a main part of the flow field near the flame front. The vortical velocity field counteracts the oscillating flow field near the curved flame front and hence stabilizes the motion of the flame at the curved region.

From the results of the numerical and experimental studies, vorticity production is found to be an decisive clue in the simulation of the curved flame motion especially in the time varying flow field.

REFERENCES

Ashurst, W. T., 1987, "Vortex simulation of unsteady wrinkled laminar flames", *Combust. Sci. and Technol.*, vol. 52, pp. 325-351.

Clavin, P. and Williams, F. A., 1982, "Effects of molecular diffusion and thermal expansion on the structure and dynamics of premixed flames in turbulent flow of large scale and low intensity", *J. Fluid Mech.*, vol.116, pp251-282.

Garcia-Ybarra, P., Nicoli, C. and Clavin, P., 1984, "Soret and dilution effects on premixed flames", *Combust. Sci. and Technol.*, vol. 42, pp. 87-109.

Ghoniem, A. F., Chorin, A. J. and Oppenheim, A.K., 1982, "Numerical modeling of turbulent flow in a combustion channel", *Phil. Trans. R. Soc. A*, vol. 394, pp. 303-325. 1982

Hayes,. W. D., 1959, "The vorticity jump across a gasdynamic discontinuity", *J. Fluid Mech.*, vol. 2, pp. 595-600,

Kerstein, A. R., Ashurst, W. T. and Williams, F. A., 1988, "Field equation for interface propagation in an unsteady homogeneous flow field", *Phys. Rev. A*, vol. 37, pp. 2728-2731.

Markstein, G. H., 1964, Nonsteady flame propagation, Pergamon Press.

Pindra, M. -Z. and Talbot, L., 1988, "Some fluid dynamic considerations in the modeling of flames",

Combustion and Flame, vol. 73, pp. 111-125.

Poinsot, T., Veynante, D. and Candel, S., 1991, "Quenching process and premixed turbulent combustion diagram", *J. Fluid Mech.*, vol. 228, pp. 561-606.

Rhee,. C. W., Talbot. L. and Sethian, J. A., 1995, "Dynamical behaviour of a premixed turbulent open V-flame", *J. Fluid Mech.*, vol. 300, pp. 87-115.

Uberoi, M. S., 1963, "Flow fields of flame propagating in channels based on the source sheet approximation", *Phys. Fluid*, vol. 6, pp. 1104-1109.

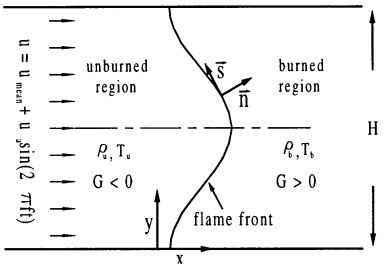

Figure 1. Problem definition and coordinate system

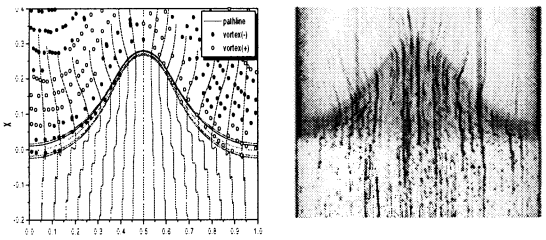

(a) numerical result (b) experimental result

Figure 2. Overall flow characteristics

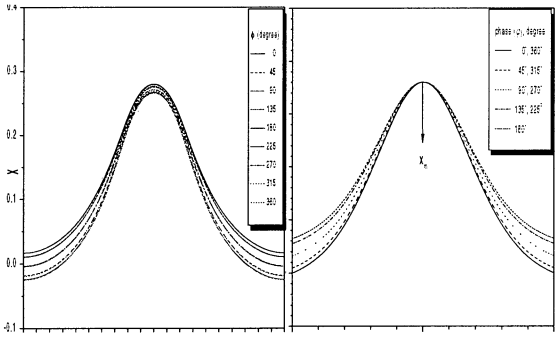

(a) numerical result (b) experimental result

Figure 3. Flame shape at various phases

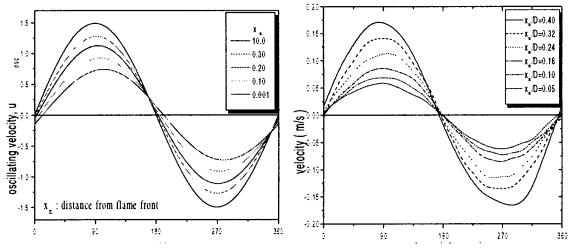

(a) numerical result (b) experimental result

Figure 4. Reduction of the oscillating velocity

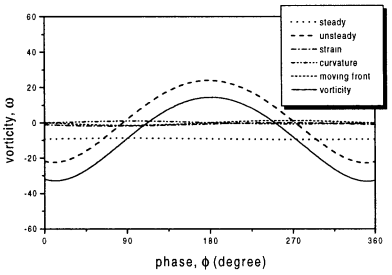

Figure 5. Vorticity production at the flame front (y=0.35)

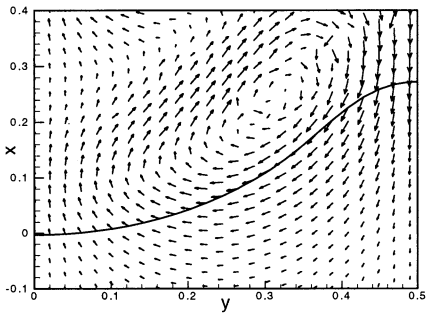

Figure 6(a). Vortical velocity field at 90°

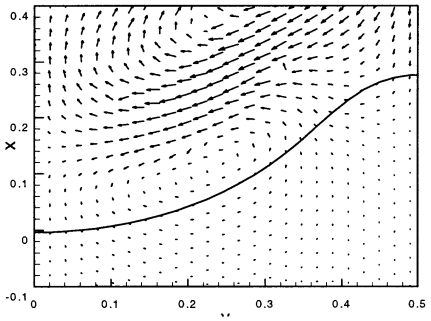

Figure 6(b). Vortical velocity field at 270°

Figure 6. Vortical velocity field at various phases